Global Nuclear Fuel

A Joint Venture of GE, Toshiba, & Hitachi

NEDO-33236
eDRF Section 0000-0046-9229
November 2005

Licensing Topical Report

GE14 Fuel Assembly Mechanical Design Report

M. DeFilippis
R. Higgins

NON PROPRIETARY NOTICE

This is a non proprietary version of the document NEDC-33236P, which has the proprietary information removed. Portions of the document that have been removed are indicated by an open and closed bracket as shown here [[ ]].

IMPORTANT NOTICE REGARDING CONTENTS OF THIS REPORT

Please Read Carefully

The information contained in this document is furnished as reference material for GE14 Fuel Assembly Mechanical Design. The only undertakings of Global Nuclear Fuel respecting information in this document are contained in the contracts between Global Nuclear Fuel and the participating utilities in effect at the time this report is issued, and nothing contained in this document shall be construed as changing those contracts. The use of this information by anyone other than that for which it is intended is not authorized; and with respect to any unauthorized use, Global Nuclear Fuel makes no representation or warranty, and assumes no liability as to the completeness, accuracy, or usefulness of the information contained in this document.

CONTENTS

FIGURES

TABLES

ABSTRACT

This document provides the results of the mechanical analyses for GE14 fuel assemblies. These results demonstrate the mechanical integrity of the fuel bundle components under various mechanical loading conditions and the adequacy for withstanding limiting structural stresses, fretting wear, and dimensional changes.

ACRONYMS AND ABBREVIATIONS

Term	Definition
AFL	Active Fuel Length
DRF	Design Record File
GWd	Gigawatt days
LEP	Lower End Plug
LTP	Lower Tieplate
MTU	Metric Tons of Uranium
PLR	Partial Length Rod
SF	Scale Factor
UEP	Upper End Plug
UTP	Upper Tieplate

1. INTRODUCTION AND SUMMARY

This report provides the results of the mechanical analysis of the GE14 fuel assembly. These results demonstrate the mechanical integrity of the fuel assembly components under various mechanical loading conditions and the adequacy for withstanding limiting structural stresses, fretting wear, and dimensional changes.

2. FUEL ASSEMBLY DESCRIPTION

2.1 Fuel Bundle

The GE14 fuel assembly, Figure 2-1, Ref. 5, consists of a fuel bundle (comprised of fuel rods, water rods, spacers, and upper and lower tieplates), and a channel that surrounds the bundle. Several significant fuel assembly parameters are given in Table 2-3. The GE14 design contains [[ ]] Figure 2-4. The fuel and water rods are spaced and supported by the upper and lower tieplates with intermediate spacing provided by [[ ]] spacers. The upper and lower tieplates are connected by [[ ]] tie rods threaded into the lower tieplate and attached by nuts at the upper tieplate. The upper tieplate has a handle for transferring the fuel bundle from one location to another. The fuel assemblies in the reactor are supported and positioned by the fuel–support casting and core plate at their lower end and positioned horizontally by the top guide at their upper end. The fuel channel provides the structural lateral stiffness to the fuel assembly. A detailed description of the specific fuel assembly components is provided in the following subsections.

2.1.1 Fuel Rods

Each fuel rod consists of high–density ceramic uranium dioxide fuel pellets stacked within Zircaloy cladding that is evacuated, backfilled with helium to [[ ]]bar, Ref. 2, 6, 7, and sealed with Zircaloy end plugs welded on each end. The innermost part of the Zircaloy cladding is replaced by a thin zirconium barrier liner that is metallurgically bonded to the base Zircaloy material during manufacture.

Adequate free volume is provided within each fuel rod in the form of a pellet–to–cladding gap and a plenum region at the top of the fuel rod to accommodate thermal and irradiation expansion of the UO_2 and the internal pressures resulting from the helium fill gas, impurities, and gaseous fission products liberated over the design life of the fuel. A compression spring is provided in the plenum space to minimize movement of the fuel column inside the fuel rod during shipping and handling operations while permitting the fuel column to expand axially during operation.

Three types of fuel rods are used in the GE14 fuel assembly: tie rods, standard rods, and partial length rods (PLRs). The tie rods in each bundle have lower end plugs that thread into the lower tieplate and threaded upper end plugs that extend through the upper tieplate. Nuts and locking tab washers are installed on the upper end plug to hold the fuel bundle together. These tie rods support the weight of the bundle during fuel handling operations when the assembly is lifted by the handle. During operation, the fuel assembly is supported by the lower tieplate. The end plugs of the standard fuel rods (Figure 2-2) have shanks that fit into bosses in the tieplates. An expansion spring is located over the upper end plug shank of each standard and tie rod in the assembly to keep the fuel rods seated in the lower tieplate while allowing independent axial expansion of the fuel rods by allowing their upper end plug shanks to slide within the holes of the upper tieplate. The GE14 fuel assembly also includes [[ ]] PLRs (Figure 2-4) that

are selectively located in the lattice to maximize fuel weight, reduce two–phase pressure drop and increase cold shutdown reactivity margins. The PLRs extend just past the top of the [[ ]] spacer and have threaded lower end plugs for attaching to the lower tieplate.

2.1.2 Water Rods

The GE14 assembly is designed with [[ ]] large circular water rods that are centrally located and occupy [[ ]] fuel rod lattice positions. A dimensional description of the water rods is included in Table 2-3. Typical spacer–positioning water rods are shown in Figure 2-3, Ref. 8, 9. The water rods are hollow Zircaloy tubes with several holes around the circumference near each end to allow coolant to flow through. An orifice contained at the lower diameter transition or in the lower reduced diameter tube controls the water rod flow. One of the [[ ]] water rods in each bundle positions the [[ ]] fuel spacers axially. This spacer–positioning water rod is designed with a square bottom end plug and with spacer positioning tabs that are welded to the tube exterior above and below each spacer location. [[ ]]non–spacer–positioning water rod has a round shank lower end plug and no spacer–positioning tabs. The spacer–positioning water rod is prevented from rotating by the engagement of its square lower end plug with a square hole in the lower tieplate. An expansion spring is located over the upper end plug shank, between the water rod shoulder and upper tieplate, to allow for differential axial expansion similar to the full–length fuel rods.

2.1.3 Spacers

The primary function of the fuel spacer is to provide lateral support and spacing of the fuel rods. The GE14 fuel uses [[ ]] spacers that have a Zircaloy cell design with [[ ]]springs. The Zircaloy spacers, Ref. 10, 11, are shown in Figure 2-5 and Figure 2-6. Cells have been removed from the three spacers above the PLRs (Figure 2-6) in the Zircaloy spacer design to minimize the two-phase pressure drop. The spacer spring forces in each design are established so as to avoid fretting wear on the fuel rods due to fuel rod vibration.

2.1.4 Upper And Lower Tieplates

[[ ]]stainless steel upper and lower tieplates carry the weight of the fuel and position the rod ends laterally during operation and handling. The upper tieplate has an internally threaded corner post, on one of the two posts that supports the channel. The threaded post accepts the channel fastener bolt. The upper tieplate has been synergistically designed with the [[ ]] large central water rods and the PLRs to maximize flow area and therefore minimize two–phase pressure drop, Ref. 12, (Figure 2-7).

The lower tieplate design, Ref. 13, (Figure 2-8) increases the single–phase pressure drop at the bottom of the bundle (relative to earlier GNF fuel designs) while providing a uniform local

bundle flow distribution and protection from debris. [[ ]] end plug hole locations are threaded to accept [[ ]] tie rods and [[ ]] PLRs. The lower tieplate also features an extended boss around each of the water rod lower end plugs. These extended bosses mitigate flow–induced vibration which could otherwise be caused by coolant impinging on the longer water rod lower end plugs. Pockets are machined in all four sides of the lower tieplate to accept finger springs. [[ ]] finger springs are employed to control the bypass flow through the channel/lower tieplate flow path over a range of channel sidewall creep deflections over lifetime. The lower tieplate casting body also has two flow holes drilled in two adjacent sides of the transition region to augment flow in the bypass region.

2.2 Processing of Zircaloy-2

GE14 fuel assemblies are fabricated in accordance with materials and processing specifications and assembly processes specification current at the time of fabrication. The GE14 fuel assembly contains water rods, spacer ferrules and channel box that are fabricated from Zircaloy-2 with [[ ]] anneals. This combination of alloy and heat treatment has been used by GNF since before the introduction of reload quantities of barrier fuel in the early 1980s. The ASTM alloy composition for Zircaloy-2 is given in Table 2-1.

Table 2-1 ASTM Alloy Composition Specification for Zircaloy-2

Element	Concentration (weight %)
Tin	1.20 - 1.70
Iron	0.07 - 0.20
Chromium	0.05 - 0.15
Nickel	0.03 - 0.08

Currently, GE14 water rods and spacer ferrules are produced by tube reduction processes and finished water rod tubes and spacer ferrules are similar to the Zircaloy-2 portion of fuel tubing in terms of alloy composition, anneal, and textures. The spacer band and channel box are produced from strip material. The channel strip is machined to produce the required thick-thin cross-section for the finished channel box, bent to produce channel halves and welded together to produce a channel box. The welded box is then thermal sized annealed to produce the final channel box. Specifications for the crystallographic texture for 100 mil thick channel strip are given in Table 2-2.

Table 2-2 100 Mil Channel Strip Nominal Crystallographic Texture

Direction	Texture Factor
Longitudinal	$0.0323 <= f_L <= 0.1103$
Normal	$0.5170 <= f_N <= 0.8030$
Transverse	$0.1100 <= f_T <= 0.4260$

Note: f_I is the fraction of basal poles in the I-direction

Periodically, GNF revises the fabrication of the Zircaloy-2 fuel assembly components or the bundle assembly process, primarily to (1) improve corrosion performance as fuel operating strategies and plant water chemistries evolve, (2) to optimize in-reactor performance of the assembly or (3) to improve the bundle assembly process. The impact of such changes on the thermal-mechanical properties used in design and licensing analyses of Zircaloy-2 fuel assembly components are assessed as follows.

The material properties of Zircaloy based fuel assembly components used in thermal-mechanical design and licensing analyses of these components include:

(1) Elastic properties (elastic modulus and Poison's ratio)

(2) Thermal expansion coefficients

(3) Plastic properties (yield and ultimate stress and failure strain)

(4) Creep properties

(5) Fatigue properties

(6) Irradiation growth properties

(7) Corrosion properties

The elastic properties and thermal expansion coefficients are only weakly dependent upon alloy composition and more dependent upon fabrication process, specifically the reduction process and the resulting texture. Since GNF has maintained essentially unchanged texture specifications on fuel assembly components, the periodic process changes will have negligible impact on these properties.

Likewise, the plastic and creep properties are only weakly dependent upon alloy composition. However, these properties are strongly dependent upon the fabrication process, specifically the final heat treatment. Since GNF assembly components are [[ ]] annealed at the end of the fabrication process, the periodic process changes will have negligible impact on these properties.

Also, the fatigue and irradiation growth properties are only weakly dependent upon alloy composition and strongly dependent upon the fabrication process, specifically the final heat treatment and texture. Since GNF assembly components are [[ ]]annealed at the end of the fabrication process and the texture specifications are essentially unchanged, the periodic process changes will have negligible impact on irradiation growth properties.

Finally, the corrosion properties have a strong dependency on fabrication process, and specifically on the in-process heat treatments. GNF has recognized this dependency and maintains an on-going program to measure and characterize corrosion performance for Zircaloy-2 fuel assembly components for a variety of operating conditions and plant water chemistries. These characterizations are used to determine corrosion statistical distributions for thermal-mechanical analyses of GNF Zircaloy-2 fuel assembly components and are updated when the data indicates an update is necessary. Thus the potential charges in corrosion performance of GNF Zircaloy-2 fuel assembly components due to both periodic process changes and changing water chemistries in the plants are directly addressed by the GNF design and licensing process.

In summary, the material properties used in GNF design and licensing analyses of Zircaloy-2 fuel assembly components adequately address periodic minor changes in the fabrication processes for these components to improve the fuel assembly processes and optimize the in-reactor performance of the GE14 fuel assemblies. If more significant process changes are made, the applicability and adequacy of the properties will be confirmed. It will also be confirmed that the impact on in-reactor performance and reliability of GE14 fuel assemblies will be acceptable.

Table 2-3 GE14 Fuel Bundle Data

Component	Units	Value
Fuel Bundle		
Fuel bundle length	mm	[[
Horizontal projection (in the channel region)	mm	
Horizontal projection (at the bottom)	mm	
Geometry		
Number of full length fuel rods		
Number of part length fuel rods		
Rod-to-rod pitch	mm	
Number of spacers		
Number of water rods		
Fuel bundle weight	Kg	
Heat transfer area	M^2	
Upper and lower tieplate material		
Maximum bundle exposure	GWd/MTU	
Maximum bundle residence time	Years	
Spacers		
Number of spacers		
Thickness of structure (Outer/Inner)	mm	
Axial spacing (from Bottom)	mm	
Structural material		
Spring material		
Spring preload nominal	N	
Water Rods		
Quantity		
Material		
Diameter	mm	
Thickness	mm	]]

Table 2-3 GE14 Fuel Bundle Data (Continued)

Component	Units	Value
Fuel Rod		
Cladding material		[[
Barrier material		
Outside diameter	mm	
Cladding thickness	mm	
Barrier thickness	mm	
Shoulder height	mm	
Shoulder height - part length rods	mm	
Active length - UO_2 rods	mm	
Active length - Gadolinia rods	mm	
Active length - part length rods	mm	
Fuel shape		
Fuel outside diameter	mm	
Density% theoretical (immersion)		
Diametral gap	mm	
Relative pellet length (L/D)		
Pellet material		
Channel		
Material		
Length	mm	
Inside width	mm	
Wall thickness of corners	mm	
Wall thickness of sides	mm	
Inside radius	mm	]]

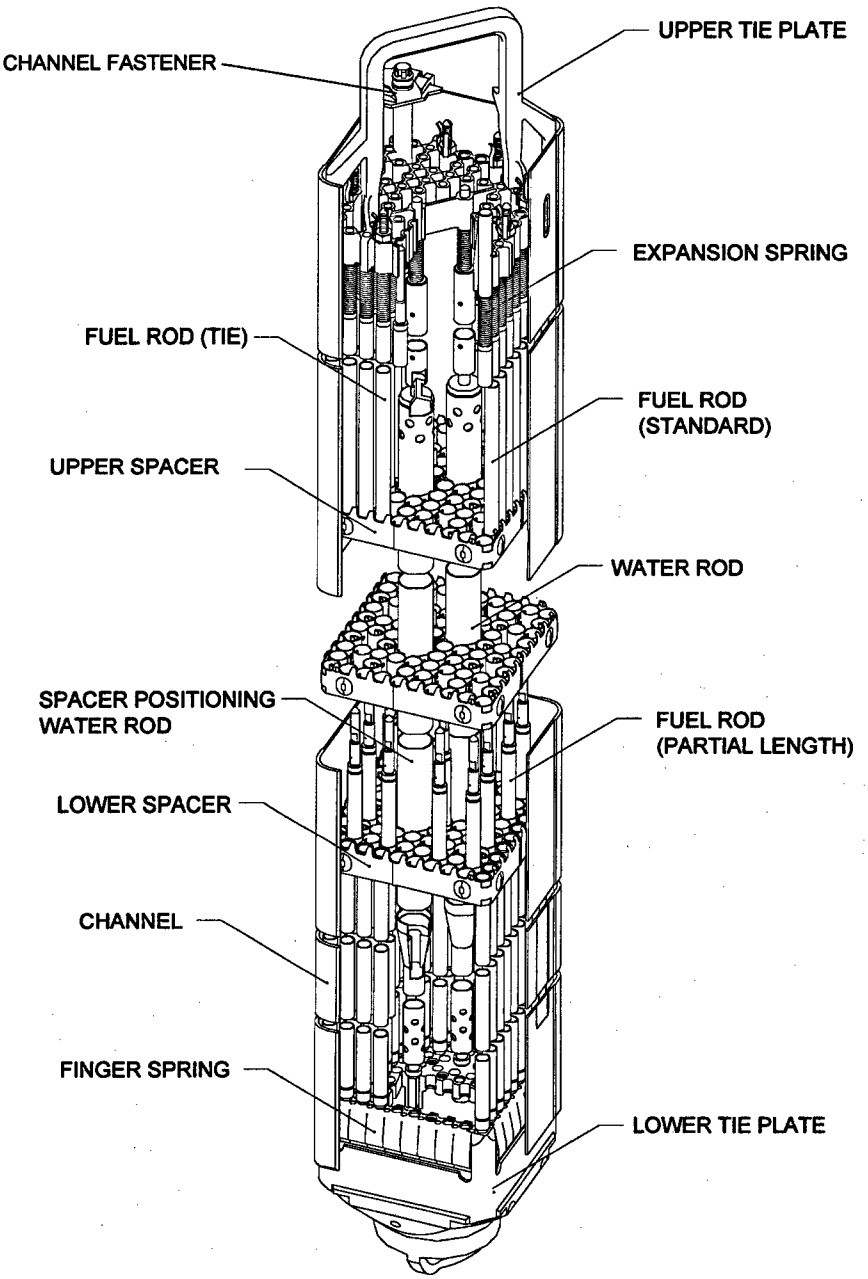

Figure 2-1 GE14 Fuel Assembly
(Ref. 5)

[[

]]

Figure 2-2 GE14 Fuel Rods
(Ref. 2, 6, 7)

[[

]]

Figure 2-3 Multi-piece and One-Piece Water Rods
(Ref. 8, 9)

[[

]]

Figure 2-4 GE14 Lattice

[[

]]

Figure 2-5 Zircaloy Spacer – Lower [[ ]] Positions
(Ref. 10)

[[

]]

Figure 2-6 Zircaloy Spacer – Upper [[ ]] Positions
(Ref. 11)

[[

]]

Figure 2-7 Upper Tieplate
(Ref. 12)

[[

]]

Figure 2-8 Lower Tieplate
(Ref. 13)

3. FUEL ASSEMBLY ANALYSIS

3.1 Compatibility/Dimensional Changes

The GE14 fuel assembly has been designed to be mechanically compatible with the reactor core configuration considering existing top guides, fuel supports, and fuel assemblies. In addition, allowances are made for dimensional changes in the fuel assembly components throughout the operating lifetime due to such considerations as irradiation growth and creep deformation. The supporting references for the calculations in the fuel assembly analysis section are contained in the associated supporting document, Ref. 0.

The design limits for acceptable component dimensional changes are as follows:

The fuel rod upper end plug initial engagement into the upper tieplate must be large enough such that at end–of–life the minimum growth fuel rod in the bundle will maintain cylindrical engagement.

The initial expansion space between the top of the fuel rod and the upper tieplate must be large enough such that at end–of–life the maximum growth fuel rod in the bundle will not compress an expansion spring beyond the solid height.

The water rod upper end plug initial engagement into the upper tieplate must be large enough such that at end–of–life the cylindrical engagement with the tieplate is maintained.

The water rod lower end plugs must be long enough to assure that they do not become disengaged from the lower tieplate should the water rod be lifted such that solid contact with the upper tieplate would occur at end-of-life.

This subsection discusses the impact of component dimensional changes on the functional capability of the GE14 assembly. The GE14 fuel assembly is designed to accommodate the differential irradiation growth that occurs between the various components of the fuel assembly. Relative to earlier GNF fuel designs, the fuel rod and water rod end plugs have been lengthened, the expansion space between the top of the rods and the upper tieplate has been increased, and the fuel channel overlap with the lower tieplate has been increased to allow for the increased differential growth which occurs at the higher discharge exposures associated with the GE14 design. The following subsections discuss the various differential growth of fuel assembly components and present evaluation results to demonstrate that adequate margin exists in the GE14 design to maintain the functional capability of the assembly when considering component irradiation growth.

3.1.1 Fuel Rod UEP/UTP Engagement and Fuel Rod/UTP Expansion Space

The fuel rod upper end plug initial engagement into the upper tieplate must be large enough such that at end–of– life the minimum growth fuel rod in the bundle will maintain engagement. This

is shown by the schematic drawing in Figure 3-1 where the minimum growth fuel rod in the bundle maintains contact between the cylindrical portion of the upper tieplate hole and the cylindrical portion of the rod upper end plug. The cylindrical engagement of the upper end plug into the upper tieplate is determined from the assembled space between the top of the fuel rod and the upper tieplate, the end plug length, and the countersink depth of the hole in the upper tieplate boss. From the dimensions given in Figure 3-1, the initial engagement of the fuel rod upper end plug is determined as follows:

Initial Engagement = [[ ]]

which gives a minimum initial engagement length of [[ ]].

The initial expansion space between the top of the fuel rod and the upper tieplate is determined by the difference between fuel bundle assembly space and the length of a fully compressed expansion spring. The expansion space is designed such that at end–of–life the maximum growth fuel rod in the bundle will not compress an expansion spring beyond the solid height. This is shown by the schematic drawing in Figure 3-2 where the fuel rod expansion space is determined as:

[[ ]]

which gives a minimum expansion space of [[ ]].

The bundle–to–fuel rod differential growth is determined from the field measurement data of bundle growth and corresponding fuel rod growth. All rods in the bundle are measured such that the true maximum and minimum rod growths are known. The maximum upper end plug disengagement and spring compression are determined for each bundle of rods measured. The data set of the worst–case rods in the bundles is plotted in Figure 3-3, (subset of Ref. 4 data). Lines representing linear fits to the data that pass through zero are also shown on Figure 3-3. The lines represent the expected worst rod in a bundle for both upper end plug disengagement and fuel rod expansion spring compression, as a function of exposure. The data in Figure 3-3 indicates that a fuel rod with minimum upper end plug engagement of [[ ]]mm at the beginning–of–life is expected to have greater than [[ ]]mm of remaining cylindrical engagement at the end–of–life ([[ ]]). Also shown in Figure 3-3, a fuel rod having the minimum expansion space of [[ ]]mm at the beginning–of–life is expected to have greater than [[ ]] mm of remaining expansion space at the end–of–life.

3.1.2 Water Rod Upper/LEP Engagement With the Upper/LTPs

The water rod upper end plug initial engagement into the upper tieplate must be large enough such that at end–of–life the cylindrical engagement with the tieplate is maintained. This is shown by the schematic drawing in Figure 3-4. From the dimensions given in Figure 3-4, the water rod upper end plug initial engagement with the upper tieplate is determined as follows:

Initial Engagement = [[ ]]

which gives a minimum initial engagement length of [[ ]]mm.

Differential growth between the fuel rods and water rods can cause the water rods to be lifted upward from their original seated positions in the lower tieplate. Thus the water rod lower end plugs must be long enough to assure that the water rods do not become disengaged from the lower tieplate. Figure 3-5 shows a water rod at end–of–life in the fully lifted position such that contact is maintained between the square lower end plug shank and the square portion of the lower tieplate hole. As shown in Figure 3-5, the water rod can be lifted upward until the large diameter portion of the upper end plug contacts the upper tieplate. The amount of lift possible is determined as follows:

Lift = [[ ]]

which gives a maximum lift value of [[ ]] mm.

The square–to–square contact initial engagement of the water rod lower end plug is determined considering the end plug shank length, the tip chamfer on the end plug, the effective depth of the square hole countersink and the seating depth of the end plug conical seat.

The water rod lower end plug initial engagement is determined from the dimensions on Figure 3-5 as follows:

Initial Engagement = [[ ]]

which gives a minimum engagement of [[ ]] mm with the conservative assumption that all calculated dimensions are independent of one another. The combination of a seated minimum initial engagement of [[ ]]mm and a maximum possible lift of [[ ]]mm gives a minimum effective engagement of [[ ]]mm.

The bundle–to–water rod differential growth is determined from the field measurement data of bundle growth and water rod growth shown in Figure 3-6, Ref. 4. The data points shown as open squares represent bundle growth measurements determined by measuring the actual distance between upper and lower tieplates of irradiated fuel assemblies. The data shown as closed diamonds represent individual water rod growth measurements. Linear relations of bundle and water rod growth as a function of exposure are determined with the results shown as the two lines on Figure 3-6. The differential growth between fuel bundles and water rods is determined as the difference between the two linear relations. This resulting linear relation for differential growth as a function of exposure is given by the sloped line in Figure 3-7. The GE14 water rod upper and lower end plug engagement lengths are shown for comparison to the predicted bundle–to–water rod differential growth value. As indicated by Figure 3-7, a water rod with minimum upper end plug or lower end plug engagement at the beginning–of–life is expected to maintain at least [[ ]] mm of engagement throughout its design lifetime.

3.1.3 Fuel Channel Overlap With the Finger Spring

Since the fuel bundle growth is controlled by the fueled tie rods, which are under tension, the fuel bundle irradiation growth will be greater than the fuel channel irradiation growth. The fuel

channel initial overlap with the finger springs on the lower tieplate must be large enough such that at end–of–life sufficient overlap of the springs is maintained. Figure 3-8 is a schematic drawing of the channel overlap with the lower tieplate and finger springs showing the channel maintaining contact over the flat portion of the finger springs at the end–of–life condition. The channel overlap of the finger springs is determined considering the dimensional stackup of the fuel rod on the lower tieplate which effectively determines the bundle length, the channel length, and the axial position of the finger spring flats relative to the lower tieplate. The amount of overlap is determined as follows:

Overlap = Channel Length – Bundle Length – Finger Spring

Channel Length = [[ ]]mm.

Bundle Length = [[ ]]

= [[ ]]mm

Finger Spring = [[ ]]mm

Overlap = [[ ]]

Minimum Overlap = [[ ]]mm

The bundle-to-channel differential growth is determined from the field measurement data of bundle growth and channel growth shown in Figure 3-9, Ref. 4. The data points shown as open squares represent bundle growth measurements determined by measuring the actual distance between upper and lower tieplates of irradiated fuel assemblies. The data shown as closed diamonds represent individual channel growth measurements. Linear relations of bundle and channel growth as a function of exposure are determined with the results shown as the two lines on Figure 3-9. The differential growth between fuel bundles and channels is determined as the difference between the two linear relations. This resulting linear relation for differential growth as a function of exposure is given by the sloped line in Figure 3-10. The GE14 channel-finger spring overlap is shown for comparison to the predicted bundle-to-channel differential growth value. The comparison indicates that the GE14 channel overlap is expected to be at greater than [[ ]]mm at the end-of-life ([[ ]] GWd/MTU).

[[

]]

Figure 3-1 Fuel End Plug Disengagement

[[

]]

Figure 3-2 Fuel Rod Spring Compression

[[

]]

Figure 3-3 Maximum Rod to Bundle Differential Growth
(Ref. 4)

[[

]]

Figure 3-4 Water Rod Upper End Plug Disengagement

[[

]]

Figure 3-5 Water Rod Lower End Plug Disengagement

[[

]]

Figure 3-6 Bundle and Water Rod Growth
(Ref. 4)

[[

]]

Figure 3-7 Bundle to Water Rod Differential Growth

[[

]]

Figure 3-8 Channel/ Finger Spring Overlap

[[

]]

Figure 3-9 Bundle and Channel Growth

(Ref. 4)

[[

]]

Figure 3-10 Bundle/ Channel Differential Growth

3.2 Design Loads

The structural adequacy of the fuel assembly components is demonstrated by evaluations (analysis or testing) that specifically address the operational duty that results from the BWR environment. This duty results from steady–state operation (including handling loads), mechanical loads associated with anticipated transients, and accident loads due to external conditions. The actual loading conditions used in the mechanical evaluations of the GE14 fuel assembly are specified in the discussions presented in Section 3.4.

3.2.1 Upper Tieplate

The design loading for the upper tieplate is from bundle handling. Specifically a load equal to three times the bundle weight is applied at the tieplate handle to grapple attachment. The load is reacted at the [[ ]]tie rod locations.

3.2.2 Lower Tieplate

The design loading for the lower tieplate is from bundle handling. Specifically a load equal to [[ ]] times bundle weight is applied uniformly to the lower tieplate grid boss locations.

3.2.3 Fuel Rod End Plug

The design loading for the fuel rod end plugs is from bundle handling. Specifically [[ ]] times the bundle weight plus the sum of all the axial expansion spring forces is applied to [[ ]] of the [[ ]] tie rods.

3.2.4 Plenum Spring

The plenum spring is designed to resist an acceleration of the fuel pellet column of [[ ]] g's while being transported without deflecting the spring more than [[ ]] mm.

3.2.5 Expansion Spring

The expansion springs are designed to resist downward forces from grappling and the weight of the suspended components (i.e., tieplate, channel, and channel fastener) while allowing expansion from irradiation growth of the individual fuel rods and considering loss of load carrying capacity resulting from irradiation induced stress relaxation.

3.2.6 Water Rod

The water rod tubing is evaluated for a steady state differential wall pressure of 1.04 bar.

The maximum load that a water rod tab can experience due to operating effects of spacer lift forces from flow or differential irradiation/thermal expansion between the fuel rods and water rods is the load required to simultaneously slide all fuel rods through a spacer.

3.2.7 Spacer

Tests are performed to demonstrate that the GE14 spacer design can withstand significant lateral loading before any significant deformation occurs.

3.2.8 Channel

The design loadings for the channel include steady state and transient operating pressure differentials.

3.3 Design Criteria

3.3.1 Stress

The fuel assembly structural components are evaluated to ensure that the components will not fail due to stresses exceeding the fuel assembly component mechanical capability. The limits are typically applied to unirradiated material conditions because irradiation increases the material strength properties. The stress limits are applicable to the combined effective stress.

For structural components the combined effective stress may not exceed the material tensile strength. These combined stress components include primary as well as secondary. If these combined stresses exceed the material yield strength then justification must be made that the resulting distortion is not significant to component performance and that cyclic loading will not cause fatigue failure.

3.3.2 Fatigue

Fuel assembly components with significant cyclic loading are evaluated to ensure that the material fatigue capability will not be exceeded. The strain-cycles diagram for Zircaloy is shown in Figure 3-11, Ref. 1.

3.3.3 Fretting Wear

Testing is performed to assure that the mechanical features of the design do not result in significant vibration and consequent fretting wear. The vibration response of a new design is compared to a design that has demonstrated satisfactory performance through discharge exposure. Specifically the GE14 design vibration response was compared to the GE6 design for this purpose.

3.4 Design Evaluation

3.4.1 Structural Results

3.4.1.1 Upper Tieplate

The material properties that are appropriate for the upper tieplate stress evaluations are:

Yield Strength = [[ ]] N/mm^2 at room temperature

Tensile Strength = [[ ]] N/mm^2 at room temperature

The limiting loading on the upper tieplate occurs during fuel handling when the fuel assembly is lifted by the grapple that is attached to the upper tieplate handle. The loads that are evaluated are conservatively established as equal to 3.0 times the assembly weight. The GE14 fuel assembly weight, which includes the fuel bundle, channel and channel fastener weights, is [[ ]] N in air.

The upper tieplate was evaluated by a finite element analysis using the ANSYS code. The model utilizes ¼ symmetry and consists of 411 elements. The finite element model is shown in Figure 3-12. Three–dimensional beam elements were used to model the upper tieplate structure. The element cross–sectional properties were calculated from the nominal drawing dimensions. Additional elements were used across the center of each boss to correctly model the boss stiffness.

An upward vertical load of 0.25 times 3.0 times the assembly weight of [[ ]] N (slightly conservative value relative to the GE14 fuel assembly weight from above) was applied at the edge of the grapple interface with the upper tieplate handle ([[ ]] mm from the center of the handle). The downward load from the channel of 0.25 times 3.0 times the GE14 channel weight of [[ ]] N was applied at the channel post location. The upward loading from the expansion springs is also modeled ([[ ]] N per boss). The remainder of the upward vertical load was reacted at the tie rod bosses, which were restrained by springs having a stiffness equal to the stiffness of a GE14 tie rod. Additional restraints were applied along the lines of model symmetry.

The maximum bending stress in the grid portion of the tieplate (corrected for minimum dimensions) based on these loadings was determined to be [[ ]] N/mm^2. The stresses are shown on Figure 3-13. The finite element analysis, using three dimensional beam elements the same as for the grid, was also used to evaluate the stresses in the handle. The maximum stress in the handle occurs at the center of the horizontal portion of the handle. Correcting the stresses for minimum material results in a stress equal to [[ ]] N/mm^2.

Testing was also performed to assure that excessive deformation or fracture would not occur. The test tieplate was mounted in a fixture with springs attached at each of the tie rod locations to simulate the axial stiffness of the fuel rods. Loads in excess of requirements were applied to the handle by a simulated grapple. Test results demonstrated that fracture or excessive deformation would not occur, Ref. 15.

These analyses and tests demonstrate that the GE14 upper tieplate will not experience excessive deformation or failure during service.

3.4.1.2 Lower Tieplate

The material properties which are appropriate for the lower tieplate stress analysis are:

Yield Strength = [[ ]] N/mm^2 at room temperature

Tensile Strength = [[ ]] N/mm^2 at room temperature

The limiting loading condition on the lower tieplate is due to seating of the fuel assembly into the core or into the fuel storage racks. The loads which are evaluated are equal to [[ ]] times the assembly weight (i.e., [[ ]]N).

The lower tieplate was evaluated by a finite element analysis using the ANSYS code. The model utilizes 1/4 symmetry and consists of 666 elements. The finite element model is shown in Figure 3-14. Three-dimensional beam elements were used to model the tieplate structure. The element cross-sectional properties were calculated from the nominal drawing dimensions.

The maximum bending stress in the grid portion of the tieplate (corrected for minimum dimensions) based on these loadings was determined to be [[ ]] N/mm^2.

This lower tieplate analysis result demonstrates that the lower tieplate stresses are well below the strength values.

3.4.1.3 Fuel Rod End Plug

The fuel rod end plug stress analysis addresses the loads associated with fuel handling operations that are the most severe loading conditions for the end plugs. The strength properties of Zircaloy at room temperature are:

Yield Strength = [[ ]] N/mm^2

Tensile Strength = [[ ]] N/mm^2

The design basis axial force acting on the end plugs is 3.0 times the bundle weight lift load plus the axial spring forces of the fuel rod expansion springs. The total force exerted by the [[ ]] fuel rod springs and [[ ]] water rod springs is [[ ]] N. It is conservatively assumed that only [[ ]] tie rods carry this axial load. Therefore, the resulting force on an end plug is:

[[ ]]

The tensile stresses in the end plug shanks due to the axial load are then calculated as:[[

]]The bending stress in the end plugs is given by: $\sigma = \frac{Mc}{I}$

where:

σ = bending stress,

M = moment,

c = distance from neutral axis to outer fiber and

I = moment of inertia.

The value of M is derived from the non–parallelism of the interfacing surfaces with the axis of the end plug shank. Therefore,
[[

]]

The effective stresses are:

[[

]]

The shear stress in the end plug threads is given by:

$$\tau = \frac{F}{\pi d_m L}$$

where:

τ = shear stress

F = axial force

d_m = minor bolt diameter

L = length of engaged threads

Therefore,
[[

]]

The effective stresses are:
[[

]]

These results demonstrate that even with conservative analysis assumptions, the stresses are well below the material strength values.

3.4.1.4 Plenum Spring

The plenum spring is designed to resist an acceleration of the fuel pellet column of [[ ]] g's while being transported without deflecting the spring more than [[ ]] mm. The spring is also designed to exert a minimum preload on the pellet column of [[ ]] N.

The maximum plenum spring stress allowable is: σ_{eff} < Yield Strength
The material properties for the [[ ]] stainless steel springs at room temperature are:

Yield Strength = [[ ]] N/mm^2

Figure 3-15, Figure 3-16 and Figure 3-17 show the important dimensions of the basic rod, gadolinia rod and part length rod plenums. The plenum springs for the different rod types use a common wire diameter and coil diameter. The plenum spring designs accommodate the different plenum lengths by using different numbers of coils and free spring lengths.

The minimum spring preload is determined from:

$$P_{min} = K_{min} (L_f - L_a)$$

where the minimum spring constant, K_{min} is specified by the plenum spring drawing.

Substituting the appropriate spring constants and spring lengths gives the minimum preload for each rod type as follows:

		Basic Rod	Gadolinia Rod	Part Length Rod
Spring Constant,	K_{min}:	[[	[[	[[
Free length,	L_f:			
Assembled length,	L_a:			
Minimum Preload,	P_{min}:	]]	]]	]]

The minimum plenum spring preload for each rod type meets the [[ ]] N criteria.

To evaluate the maximum fuel column deflection of [[ ]] mm under the [[ ]] g loading criteria, the following equation is used:

$\delta = 0$ if [[,]]otherwise [[ ]]

where:

δ = the fuel column deflection

W = the fuel column weight

P = the initial spring preload

K = the spring stiffness.

Substituting the appropriate values for fuel column weight, spring constant and preload for each rod type gives the maximum fuel column deflection as follows:

	Basic Rod	Gadolinia Rod	Part Length Rod
W:	[[	[[	[[
P_{min}:			
K_{min}:			
δ:	]]	]]	]]

The deflections are less than the [[ ]] mm maximum deflection criteria for the [[ ]] g loading.

Stresses are evaluated for the condition of maximum spring preload, i.e., minimum plenum length and maximum spring stiffness. The relations and values used to determine the maximum plenum spring stresses are:

$$P_{max} = K_{max} (L_{fmax} - L_{amin})$$

$$\tau = \frac{8PD}{\pi d^3} K_W$$

where K_W = curvature correction factor.

$$K_W = \frac{4\left(\frac{D}{d}\right) - 1}{4\left(\frac{D}{d}\right) - 4} + \frac{0.615}{\left(\frac{D}{d}\right)}$$

where for each fuel rod type:

d = [[ ]] mm

D = [[ ]] mm.

Substituting the appropriate values for the spring and plenum designs gives the maximum plenum spring preload and stress for each rod type as follows:

	Basic Rod	**Gadolinia Rod**	**Part Length Rod**
K_{max}:	[[	[[	[[
L_f:			
L_a:			
P_{max}:			
K_W:			
τ:			
σ_{eff}	]]	]]	]]

The stress limit for the plenum spring is [[ ]] N/mm^2. The maximum plenum spring stresses are less than the limit.

3.4.1.5 Expansion Spring

The material properties for the Alloy [[ ]] expansion springs that are appropriate for this analysis are:

Tensile strength = [[ ]] N/mm^2 at room temperature

Tensile strength = [[ ]] N/mm^2 at 288 °C

G=[[ ]] N/mm^2 at room temperature

G=[[ ]] N/mm^2 at 288 °C

$$\tau = \frac{K_W G d}{\pi N D^2}(L_f - L_a)$$

$$K_W = \frac{4\left(\frac{D}{d}\right)-1}{4\left(\frac{D}{d}\right)-4} + \frac{0.615}{\left(\frac{D}{d}\right)}$$

where:

d = [[ ]] mm

D = [[ ]] mm

N = [[ ]]

K_W = [[ ]]

L_f = [[ ]] mm

L_a = [[ ]] mm

at room temperature τ = [[ ]] N/mm^2

σ_{eff} = [[$\sqrt{3}$]]N/mm^2

at 288 °C τ = [[ ]] N/mm^2

σ_{eff} = [[$\sqrt{3}$]]N/mm^2

The effective stress at room temperature, [[ ]] N/mm^2, and at operating temperature, [[ ]] N/mm^2, are significantly below the corresponding tensile strengths of [[ ]] N/mm^2 at room temperature and [[ ]]N/mm^2 at operating temperature.

3.4.1.6 Water Rod

The water rod tubing was evaluated for a steady state differential wall pressure of [[ ]] bar. The Zircaloy material properties for this operating condition, which are appropriate for this analysis, are:

Yield Strength = [[ ]] N/mm^2

Tensile Strength = [[ ]] N/mm^2

The material properties shown are conservatively low because they are applicable to a temperature of 343°C rather than the operating temperature of 288°C.

The water rod tube membrane stress was determined from:

$$S = Pr/t$$

where:

S = membrane stress

P = pressure differential

r = mean tubing radius

t = tubing wall thickness

The maximum stress occurs in the large diameter portion of the water rod. Therefore, [[ ]]

which is well below the material strength properties.

The shear strength of the welded water rod tabs is defined by the water rod drawing to be a minimum of [[ ]] N. Because the strength specified is applicable at room temperature, a load Scale Factor (SF) is used to account for the strength of the material at operating conditions. The Scale Factor used is the ratio of the tensile strengths of the Zircaloy material at room temperature to that at 288 °C. These values are [[ ]] and [[ ]] N/mm^2.

[[ ]]

The Scale Factor is conservatively high because the material properties used for operating temperature are applicable to 343°C rather than 288°C. The minimum load capability of the welded water rod tab at operating temperatures is, therefore, [[ ]] N.

The maximum load that a water rod tab could experience due to operating effects of spacer lift forces from flow or differential irradiation/thermal expansion between the fuel rods and water

rods is the load required to simultaneously slide all fuel rods through a spacer. The load required to slide a spacer along all the fuel rods of a bundle was measured for a previous 8x8 lattice design to be [[ ]] N. Because the GE14 spacer springs have the same preload as the previous spacer design springs, the friction load per fuel rod will be similar for the two designs. The GE14 spacer total load will be larger by the proportionally greater number of fuel rods in the bundle making the GE14 spacer load approximately [[ ]] N. Therefore, the water rod tab has a substantial margin to the maximum operating load.

[[ ]]

3.4.1.7 Spacer

Tests have been performed to demonstrate that the two GE14 spacers can withstand significant loading before any significant deformation occurs, Ref. 16. The tests were performed by assembling a test spacer onto a short section of a fuel bundle with empty fuel rods. The ends of the fuel rods were held in place by fixed lower tieplates. The test spacer was loaded by a section of fuel channel, which was attached and driven by the hydraulic piston of a tensile machine. Cyclic loading at a rate of 10 to 20 cycles/minute was applied by the channel section to the spacer bands with the load reacted onto the individual fuel rods in each spacer cell. Figure 3-20, Figure 3-21 and Figure 3-22 show the test configuration. This type of loading simulates the spacer reaction to fuel rod inertial loading due to a side load being applied to the fuel bundle. Since the tests were performed at room temperature, a load scale factor was used to account for the strength of the material at operating conditions. The Scale Factor used was the ratio of the yield strength of the Zircaloy at room temperature to that at 288°C.

The [[ ]]-cell spacer is the design used for the bottom five spacers of the GE14 fuel bundle. The [[ ]]-cell spacer is used for the top three spacer locations where the absence of the [[ ]] part length rods reduces the number of cells required to support the fuel rods. The spacers tested were in the "as-built" nominal thickness condition of [[ ]] mm cells and [[ ]] mm bands. Testing nominal thickness spacers is the standard practice for deformation testing since the limiting conditions are at beginning-of-life before any material strength benefits are gained from irradiation hardening of the Zircaloy material.

Figure 3-18 shows a GE14 [[ ]] cell spacer that was tested to a load of [[ ]]N without visible distortion. Figure 3-19 shows a GE14 [[ ]] cell spacer that was tested to a load of [[ ]]N without visible distortion.

3.4.1.8 Channel Stress Analysis

The analysis condition for the channel is a channel wall differential pressure of [[ ]] bar.

The Zircaloy yield strength at 288°C that is appropriate for this analysis is:

Yield strength = [[ ]] N/mm^2

The channel stresses due to this pressure gradient were determined by a finite element analysis. The model utilizes 1/8th symmetry and is shown in Figure 4-2.

The maximum bending stress occurs in the channel corner.

σ_B max = [[ ]] N/mm^2

The stress is tensile on the inside and compressive on the outside at this location.

The resulting effective stress is [[ ]] N/mm^2, which is well below the yield and ultimate material strength values.

3.4.1.9 Channel Lateral Loading Capability

Thick corner thin sidewall channels were tested to determine the allowable transverse bending load that could be sustained without buckling or collapsing the channel. The test configuration is shown in Figure 3-23. The test channel was simply supported at each end in the fixture. Three hydraulic actuators were used to produce the correct moment and shear in the middle region of the channel where buckling would occur. Channels were tested in the lateral and diagonal loading directions. Test results showed that the thick corner thin sidewall channel design has a buckling capability that exceeds design basis loads, Ref. 3.

3.4.1.10 Flow-Induced Vibration

The GE14 fuel assembly was tested to assure that the new features do not result in a significant increase in flow induced vibration (FIV) response and increase the potential for fretting wear. This testing specifically addressed such features as the water rod and extended lower tieplate boss, the part length rods, the spacer design and the lattice configuration. These features have been used successfully in prior GNF lead use assemblies. The water rod lower end plug/extended boss configuration for both round and square end plugs has been a production feature of GNF fuel designs since 1983.

The method used to demonstrate the FIV acceptability of the GE14 fuel assembly is to compare the vibration response of the GE14 design with the GE6 design. If the GE14 response is not significantly different than the GE6 response, then the FIV behavior of the GE14 design is acceptable. The GE6 fuel assembly's FIV performance is considered acceptable based upon its performance in reactor operation. The GE14 fuel rod response was measured at several locations, Ref. 20. The GE6 bundle was then inserted in the test loop and comparable locations were evaluated at the same flow conditions and with the same instrumentation. The instrumentation includes biaxial accelerometers that are mounted inside the fuel rods. The fuel rods were made up of lead, tungsten and molybdenum pellets to properly simulate the mass. Data reduction included peak acceleration and RMS displacement comparisons at a low pass filter setting of 300 Hz. The acceleration response was also double integrated to give an amplitude prediction. Response spectrums were generated to assure that there were no significant differences in response.

The results of the FIV tests show that there are no significant differences in the GE14 fuel and water rods compared to the performance of the GE6 fuel and water rods. The GE14 FIV test results also demonstrate the acceptable performance of the part length fuel rods and the large central water rods, including the water rod diameter transitions. The differences in fuel rod,

lower tieplate, spacer, and upper tieplate designs do not have a significant effect on FIV performance. These data and conclusions are therefore directly applicable to the GE14 design.

3.4.1.11 Seismic/Dynamic Loading

The GE14 fuel assembly has been designed to comply with the loading envelope and methods requirements stipulated in NEDE 21175–3–P–A, *BWR Fuel Assembly Evaluation of Combined SSE and LOCA Loadings (Amendment No. 3)*, Ref. 18.

The structural capability of the GE14 fuel assembly for withstanding seismic/dynamic loading is primarily determined by the channel and spacer designs. The channel and spacer design have been tested to assure adequate capability.

The horizontal dynamic response of the core is controlled primarily by the mass and stiffness of the fuel assemblies. The mass and stiffness properties of the GE14 fuel assembly design are not significantly different from earlier GNF fuel designs.

The vertical dynamic response and fuel lift analysis are based on a full core loading of the particular fuel design. The GE14 fuel assembly design is dynamically similar to the earlier GNF fuel designs. Prior to insertion of a full reload of GE14 the vertical dynamic/fuel lift analyses will be evaluated based of plant-specific loads such as was done in Ref. 19.

[[

]]

Figure 3-11 Zircaloy Fatigue Curve
(Ref. 1)

[[

]]

Figure 3-12 Upper Tieplate Finite Element Model

[[

]]

Figure 3-13 Upper Tieplate Bending Stress

[[

]]

Figure 3-14 Lower Tieplate Finite Element Model

[[

]]

Figure 3-15 Basic Fuel Rod Plenum

[[

]]

Figure 3-16 Gadolinia Rod Plenum

[[

]]

Figure 3-17 Part Length Fuel Rod Plenum

[[

]]

Figure 3-18 Tested Zircaloy Lower Spacer

[[

]]

Figure 3-19 Tested Zircaloy Upper Spacer

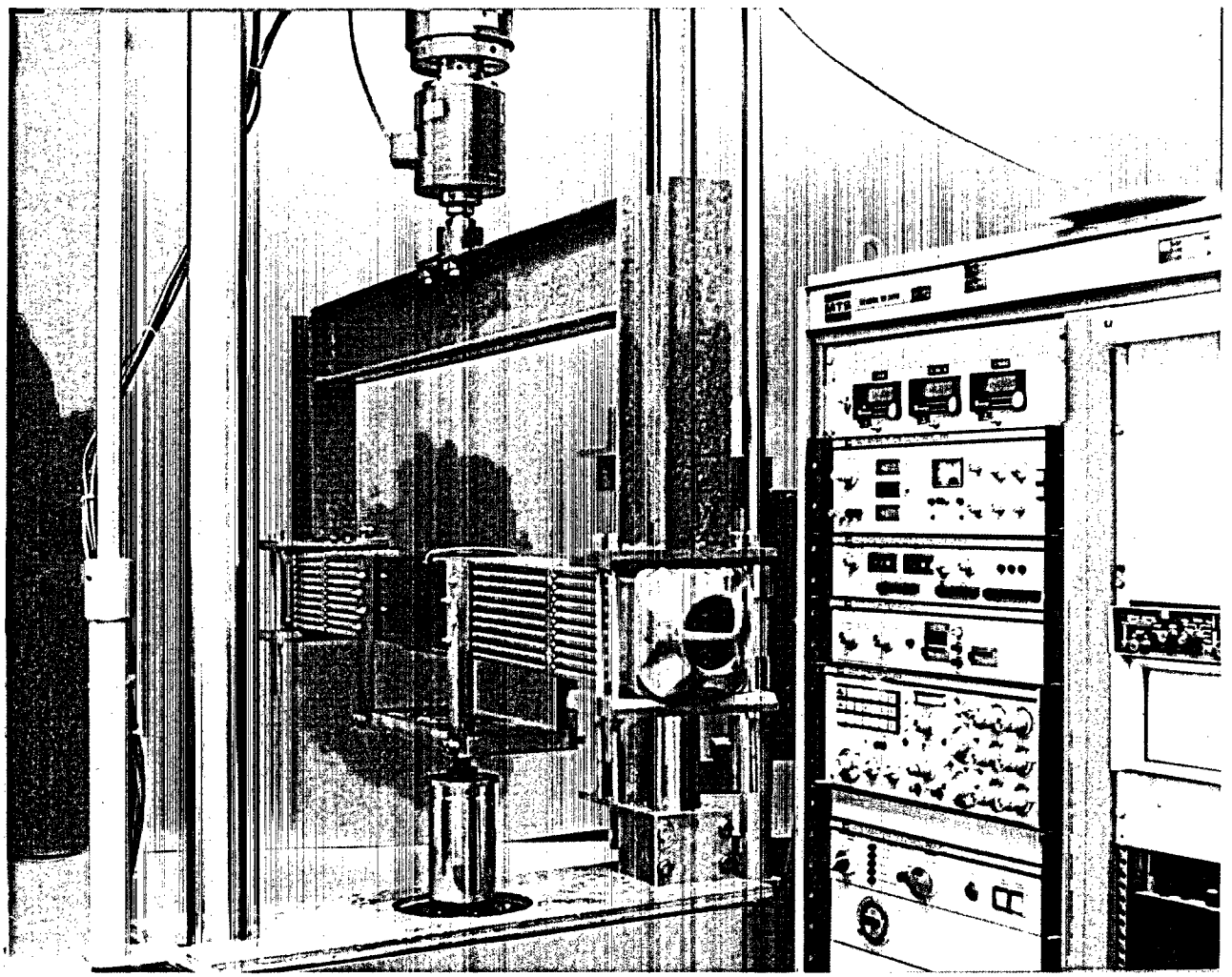

Figure 3-20 Spacer Test Fixture – Lateral Loading

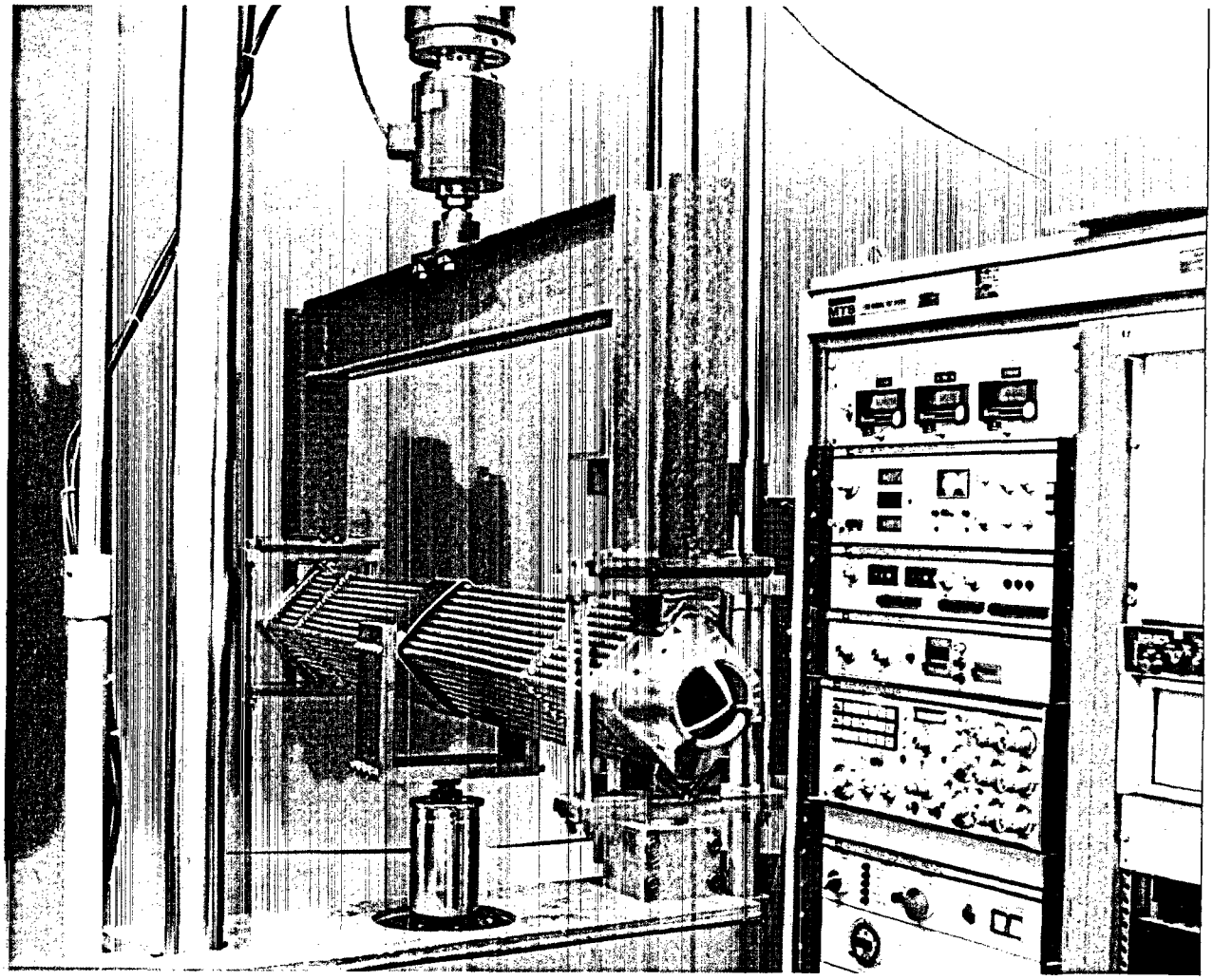

Figure 3-21 Spacer Test Fixture – Diagonal Loading

[[

]]

Figure 3-22 Spacer Test Fixture – Dummy Bundle

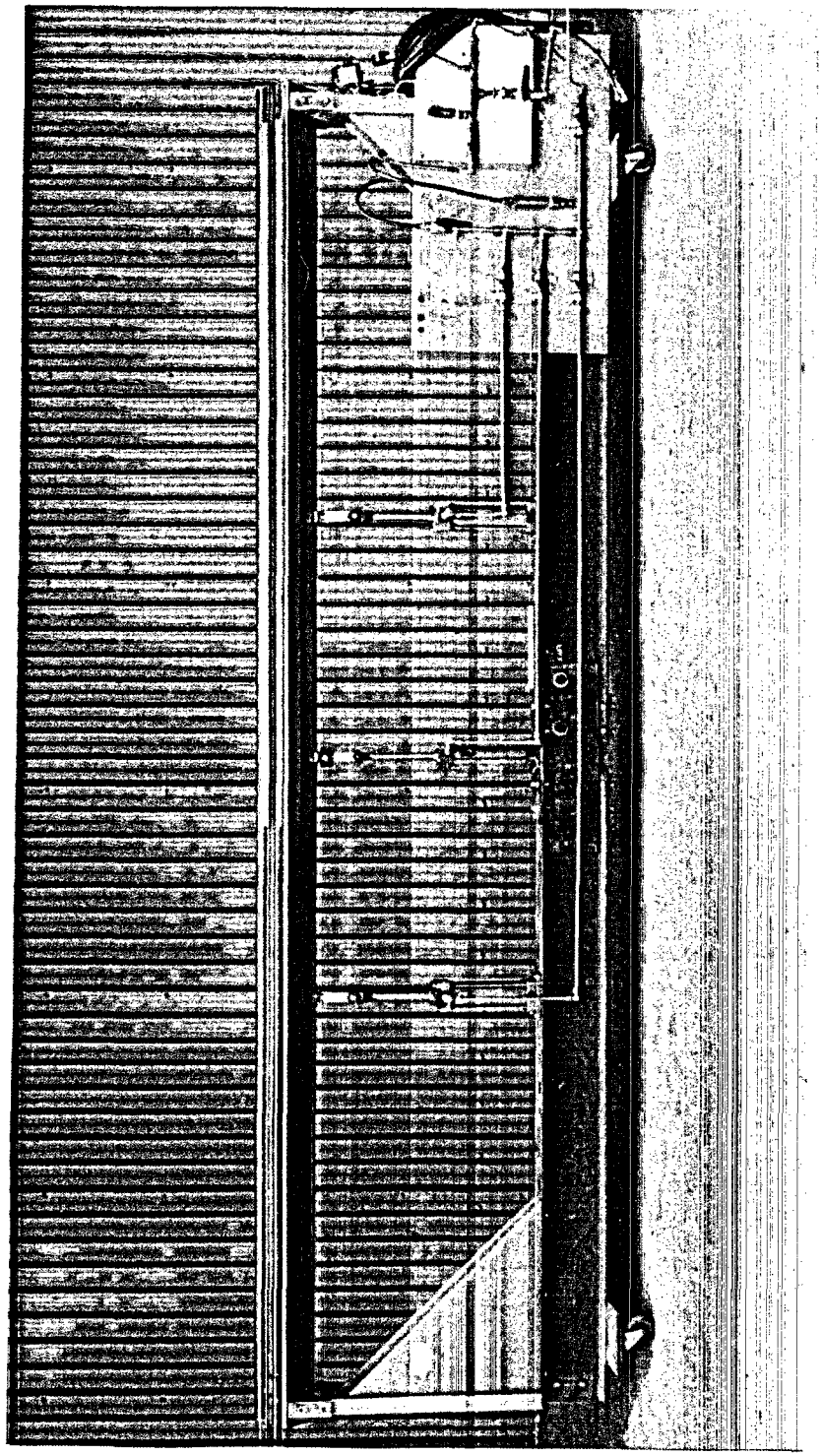

Figure 3-23 Channel Buckling Test Fixture

4. FUEL CHANNEL AND CHANNEL FASTENER

4.1 Design Description

4.1.1 Fuel Channels

The GE14 Zircaloy–2 fuel channel (Figure 4-4) performs the following functions:

1. forms the fuel bundle coolant flow path outer periphery,
2. provides a surface for control rod guidance in the reactor core,
3. provides structural lateral stiffness to the fuel bundle,
4. controls, in conjunction with the finger springs and lower tieplate, coolant bypass flow at the channel/lower tieplate interface,
5. provides a heat sink during a loss–of–coolant accident, and
6. provides a stagnation envelope for in–core fuel sipping.

The channel is open at the bottom and makes a sliding seal fit on the lower tieplate surface. At the top of the channel, two opposite corners have welded tabs, one with a hole to attach the channel to the fuel bundle. These tabs support the weight of the channel on the upper tieplate posts.

The channel design incorporates thick corners with thin side–walls to provide sufficient strength in the regions of highest stress while minimizing material for neutron economy

4.1.2 Channel Fastener

The GE14 channel fastener assembly consists of a stainless–steel casting, a one piece Alloy [[ ]] leaf spring with two active leaves at right–angles, a spring lock washer, and a fastener bolt to attach the fuel channel to the upper tieplate. The channel fastener assembly is illustrated in Figure 4-1, Ref. 14.

The channel fastener casting fits over the top of the channel and bolts through the channel clip into the upper tieplate. The casting serves as a reaction support for the leaf springs, provides a captive housing and lead-in for the fastener spring, and protects the springs from being overstressed.

The springs push the fuel assemblies apart and into the corners of the top guide cells. The spring lock washer keeps the fastener bolt from working loose after torquing into the fuel bundle. The fastener bolt is designed to attach the channel to the bundle and to remain captive in the casting.

4.2 Fuel Channel Compatibility

The GE14 fuel channel interface drawing is shown in Figure 4-4. Figure 4-5 provides dimensions for demonstrating channel compatibility with the control blades. Operational deflections associated with channel creep and deflection (bulge) and bow will influence the fitup between the channel and the control blades. The reduced side–wall thickness in the GE14 channel design ([[ ]] mm), relative to a [[ ]] mm channel design, results in greater channel bulge. However, the GE14 channel profile creates an additional [[ ]] mm ([[ ]] mm – [[ ]] mm) gap between the control blade and channel to accommodate increased bulge in the controlling fit up region of the channel/control blade.

At end of life, the mid–span deflection is the sum of the elastic deflection and the creep deflection. The elastic deflection varies with axial position according to the pressure difference acting on the channel at each axial position. The creep deflection depends on both the pressure difference and the fast fluence. Because the variation of fast fluence with axial position is not the same as the variation of pressure difference, calculations were made at several axial locations to find the maximum total deflection. Figure 4-3 shows the relation between the channel bulge deflection and exposure for the GE14 channels, Ref. 21. The deformations are calculated by finite element analyses using the 1/8 symmetry model shown in Figure 4-2. The axial location of maximum deflection is analytically determined using an axial pressure profile which is normalized to a constant lifetime pressure of [[0.65]] bar at an axial location of approximately one meter from the bottom of the channel and from a constant over lifetime flux which is developed from an axial end of life fluence profile which yields a bundle average exposure of [[ ]] GWd/MTU.

The magnitude of fuel channel bow is primarily dependent on operational effects (e.g. fluence gradients) and is independent of channel wall thickness variations. Tests have been performed which show that significant interference between control blade and channels can be tolerated without causing a failure of the control blade to settle and without significantly affecting scram times, Ref. 17.

[[

]]

Figure 4-1 Channel Fastener Assembly
(Ref. 14)

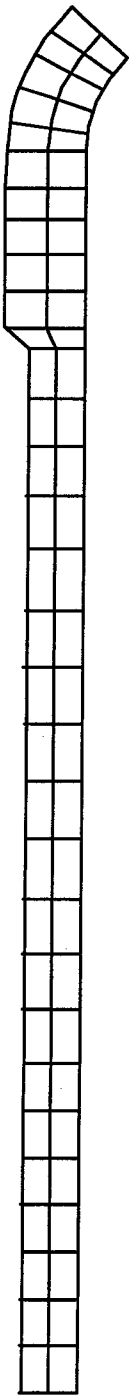

Figure 4-2 Channel Finite Element Model

[[

]]

Figure 4-3 Channel Lateral Deformation

[[

]]

Figure 4-4 Channel Compatibility

[[

]]

Figure 4-5 Channel Control Rod Compatibility

5. REFERENCES

1. Zirconium Alloys Fatigue Design Curve, Y1002C200 Rev. 6, GE Fuel & Control Materials Properties Handbook
2. 217C1442 Rev. 4, Rod, Assembly (Basic and Gad)
3. DRF J11-03430 Study 4, GE14 Channel Evaluation for Primary Loads, C.S. Chen, 8/20/98
4. eDRF section 0000-0015-5839, GNF2 Differential Growth Analysis, R. Higgins, April 16, 2003
5. 107E1591 Rev. 2, Bundle, Mechanical
6. 217C1443 Rev. 4, Rod, Assembly (Tie)
7. 217C1444 Rev. 4, Rod, Assembly (Partial)
8. 107E1583 Rev. 5, Rod, Water (Multi-piece)
9. 107E1740 Rev. 3, Rod, Water (One-piece)
10. 107E1175 Rev. 8, Spacer, Fuel (Lower 5 positions)
11. 107E1176 Rev. 10, Spacer, Fuel (Upper 3 positions)
12. 107E1016 Rev. 3, Tie Plate, Upper
13. 107E1404 Rev. 4, Tie Plate, Lower
14. 137C9004 Rev. 3, Fastener, Channel
15. DRF J11-01653 study 5.1, GE12 Upper Tie Plate (UTP) 3g Lift Test Data Tabulation, V. Hazel, June, 1993
16. DRF J11-03418, GE12/14 Spacer Seismic Test, C.F. Laing, 8/19/00
17. DRF J11-03987, Clinton Cycle 7 Channel Bow (PRC01-15), R. Rand, 9/12/01
18. NEDE-21175-3-P-A, BWR Fuel Assembly Evaluation of Combined Safe Shutdown (SSE) and Loss-of-Coolant (LOCA) Loadings (Amendment No. 3), October 1984
19. DRF B13-01980-27, GE14 Assessment Calculation Package, September 1999
20. DRF J11-03340, GE14 FIV Test, R. Strine, 3/29/98
21. DRF J11-03030, GE12 Fuel Assembly Design for TVO, R. Higgins, 1/7/99

5. REFERENCES Continued

22. eDRF Section, 0000-0046-9229, NEDC-33236P GE14 Mechanical Calculations, M. DeFilippis, 11/16/2005